



# **Effect of Atmospheric Stability on the Wind Resource extrapolating models for large capacity Wind Turbines: A Comparative Analysis of Power Law, Log Law and Deaves and Harris model**

<sup>1</sup>Pramod Kumar Sharma, <sup>2</sup>Vilas Warudkar, <sup>3</sup>Siraj Ahmed

<sup>1</sup>Research Scholar, Department of Mechanical Engineering, M.A.N.I.T, Bhopal [M.P] India

<sup>2</sup>Assistant Professor, Department of Mechanical Engineering, M.A.N.I.T, Bhopal [M.P] India

<sup>3</sup>Professor, Department of Mechanical Engineering, M.A.N.I.T, Bhopal [M.P] India

\*Corresponding author: sharma786pramod@gmail.com

Telephone Number : +91 7554051611, +91 7554051616

Fax : +91 7552670562

## **Abstract**

To observe accurate wind climate from the available met mast measured wind data at different heights an accurate wind shear model is necessary. Since WAsP and windPRO is software package which provide the better representation of wind profile over homogenous terrain only. Though, a separate module named as WAsP CFD has been added in both of the software to predict correct wind resource in complex terrain also. Now days terrain dependent wind resource model has been become a key issue for the researchers. Out of many wind extrapolating model such as PL (power law), LogL (log law), LogLL (Log linear law) and Deaves and Harris Model Log law was found to be better representation of wind profile. This study presents a comparative analysis of three different wind extrapolation models. Based on one year (2015-2017) wind data from met mast of 10min. interval at 10, 50, 80, 100 and 102m, and the result was compared with the relation of atmospheric stability. The licensed version of WAsP and windPRO software was also used to calculate wind resource parameter such as roughness index and roughness class etc. RMSE and NRMSE was found to be least in case of log linear model which is 0.11 and 0.01784 respectively in compare to PL and Deaves and Harris models.

**Keywords-** ABL, LIDAR, Monin-Obukhov length, Richardson Number, WAsP, windPRO



36

37

## Nomenclature

38

### Abbreviations

39	WT	wind turbine
	WAsP	Wind Resource Analysis and Application Programme
40	windPRO	Wind Energy Project Design and Planning
	PL	Power law
41	LogL	Log linear law
	ABL	Atmospheric Boundary Layer
42	MOST	Monin-Obukhov similarity theory
	LogLL	log-linear law
43	MLM	Maximum likelihood method
	MMLM	Modified Maximum likelihood method
44	Ri	Richardson number
	CFD	Computational fluid dynamics
45	LIDAR	Light Detection and Ranging
46	PD	Panofsky and Dutton (PD) model

### Variables

47	$v$	wind speed [m/s]
48	$k$	shape factor
	$c$	size factor [m/s]
49	$u^*$	friction velocity [m/s]
	$z_o$	roughness length [m]
50	$K$	von Karman's constant (assuming 0.4)
	$L$	Monin-Obukhov length [m]
51	$\rho$	air density [ $\text{kg/m}^3$ ]
	$C_p$	specific heat at constant pressure
52	$H$	sensible heat flux [ $\text{k. m.s}^{-1}$ ]
53	$T$	temperature in Kelvin [K]
	$\Phi_m$	Monin-Obukhov stability function
54	$\alpha$	wind shear exponent
	$v_g$	geostrophic wind speed [m/s]
55	$h$	atmospheric boundary layer height [m]
56	$f$	coriolis parameter [ $\text{s}^{-1}$ ]

### Statistical parameter

57	$n$	total number of measured /or calculated data
58	$m$	number of measured data
	$c$	number of calculated data
59	$\mu_m$	$\overline{m_i}$ mean of $n$ measured values
	$\sigma_m$	standard deviation of $n$ measured values
60	$\mu_c$	$\overline{c_i}$ mean of $n$ calculated values
	$\sigma_c$	standard deviation of $n$ calculated values
61	RMSE	root mean square error



## 62 1. Introduction

63 2015 marks the end of the beginning for the low carbon economy. As per the report of REN21 Global Status Report  
 64 (GSR) 2016, 173 countries across the world launched the target policy, 110 countries had in place either feed in  
 65 policy. Accurate measurement of wind resource is necessary to erect any wind farm. Earlier method uses cup  
 66 anemometer and wind Vane to measure the wind velocity and direction IEC. Due to advancement of Wind Power  
 67 technology attention of researchers had turned to increase the hub height. To measure the wind data at more than  
 68 100 m height by using conventional method through met mast is now becoming the costly and time consuming  
 69 process. (Henry W. Tieleman, 2008) compared the observations from power law, logarithmic law and Deaves and  
 70 Harris model in terms of mean wind speed and turbulence intensity. At 10m height non neutral thermal stability  
 71 affects the wind velocity profile and should not be neglected. (Daniel R. Drew et.al., 2013) found to be best fit non  
 72 equilibrium deaves and harris wind speed profile model in urban areas. (Hideki Kikumoto et.al., 2017)  
 73 investigated the accuracy of wind speed measurement using PL in low speed region. The results were  
 74 compared and analyzed with Doplar Lidar and ultrasonic measured wind data in the urban boundary layer of  
 75 Tokyo Japan. (Nicholas J. Cook, 1997) compared the wind speed profile with the power law and DH. The D&H  
 76 model fitted the profile near the ground and top of the ABL due to satisfying the criteria of both boundary  
 77 conditions. (Giovanni Gualtieri, Sauro Secci, 2011) compared and investigated the accuracy of prediction of wind  
 78 speed over a flat and rough region at 10m and 50m height agl in which the role of atmospheric stability and surface  
 79 roughness had discussed. (Giovanni Gualtieri, 2016) had investigated the time varying relation of wind  
 80 exponent with atmospheric stability. The model was compared with PD and found to be finest and accurate  
 81 approach in terms of wind speed profile and energy yield calculation in neutral conditions. A number of  
 82 equilibrium wind speed model namely as PL, LogL and DH had been discussed by (Davenport, 1960; Simiu and  
 83 Scanlan, 1996; Deaves and Harris, 1978). Panofsky and Dutton (1984) and Elliott (1958) studied the effect of  
 84 inner boundary layer with a step change in surface roughness for the wind urban wind profile predictions.  
 85 Deaves (1981) had utilized the concept for heterogeneous terrain and this was adapted into UK wind loading  
 86 code also. (Giovanni Gualtieri, 2017) tested and compared the DH model with PL with all stability conditions.  
 87 The DH model found to be best fitted and tuned and its accuracy seems to be increased with height from 80m  
 88 to 140 agl. Due to increasing demand of energy, Wind resource prediction has become a crucial issue markedly for  
 89 energy investors to accurately analyze the wind speed at different hub height of WT. This is very much necessary  
 90 during the feasibility study to abate the cost of wind farm installation. There are many researchers who worked on  
 91 different wind extrapolating models such as PL, LogL, LogLL and DH. Every model has its own significance and  
 92 assumptions depending upon the type of terrain where wind speed has to be predicted. (Sharma et. al. 2014) had  
 93 optimized 150m higher wind monitoring tower using ANSYS for Indian Condition. (Sharma et. al. 2014) Further the  
 94 work had extended had discussed the incorporation of advance piezoelectric and nana composite material for hybrid  
 95 offshore tower material.



## 98 2. Wind Profile extrapolating models

99 First time originally power law was proposed for the purpose of designing the wind load especially in structural  
 100 engineering (Davenport, 1960). Due to simplicity of PL model which can be applied to larger height in compare to  
 101 logarithmic law (Counihan, 1975) subjected to various terrain conditions. Following models had been generally  
 102 adopted for the wind profile predictions under certain assumptions:

### 103 2.1 Deaves and Harris (D&H) model

104 This model was developed in two stages in strong wind conditions. In the first stage it was developed for the ABL in  
 105 equilibrium over uniform roughness and in the second stage to account for multiple step changes in roughness. The  
 106 model was further developed to different kind of heterogeneous terrain. UK, Australia and New Zealand had  
 107 adapted this model into its wind design codes. If  $u_*$  is the friction velocity,  $k$  is the von karman constant (assumed  
 108 0.4),  $z_0$  is the roughness length,  $h$  is ABL height than velocity  $v$  has been define as:

109 The D&H model is also known as “logarithmic with parabolic defect” speed profile equation:

$$110 \quad V = \frac{u_*}{k} \left[ \ln \frac{z}{z_0} + 5.75 \left( \frac{z}{h} \right) - 1.88 \left( \frac{z}{h} \right)^2 - 1.33 \left( \frac{z}{h} \right)^3 + 0.25 \left( \frac{z}{h} \right)^4 \right] \quad (1)$$

$$111 \quad h = \frac{u_*}{6f} \quad (2)$$

112 where,  $f$  is the coriolis factor which depend on the site latitude angle. The extended model of D&H with step change  
 113 in roughness had been given the concept of transition from outer and inner boundary layer. It is described as:

$$114 \quad u_{*,inner} = u_{*,outer} \left[ 1 - \frac{\ln \left( \frac{z_{0,outer}}{z_{0,inner}} \right)}{0.42 + \ln m_0} \right] \quad (3)$$

$$115 \quad m_0 = \frac{0.32 X}{z_{0,inner} (\ln m_0 - 1)} \quad (4)$$

116  $X$  is the downward distance towards the change in surface roughness and  $m_0$  is the constant parameter.

117  
 118 As per Similarity theory,

$$119 \quad \frac{V}{u_*} \cong \frac{1}{k} \ln \left( \frac{z}{z_0} \right) \text{ when } z \cong h \quad (5)$$

$$120 \quad V \rightarrow V_G \text{ and } \frac{dV}{dz} \rightarrow 0 \text{ as } z \rightarrow h \quad (6)$$

121  $V_G$  Stands for the geostrophic wind speed satisfies the criteria of upper and lower boundary conditions to the ABL.  
 122 Geostrophic wind speed calculated when the thermal flux generated by the heat and friction are equal.

### 123 2.2 Log- Law model

124 The log law model was derived from Eq. (5) and holds over a ground surface:

$$125 \quad V = \frac{u_*}{k} \ln \left( \frac{z}{z_0} \right) \quad (7)$$

126 It is clear from Eq. (7) that log law satisfies the lower boundary conditions only not the upper one. Typically it had  
 127 been found to poor model for a height greater than 200m.

### 128 2.3 Power law model



129 The wind speed at a height  $z$  uses the empirical formula:

$$130 \quad \frac{V}{V_{ref}} = \left( \frac{z}{z_{ref}} \right)^\alpha \quad (8)$$

131  $V_{ref}$  to the wind speed at the height say  $z_{ref}$ . Power law indicates the increment of surface wind speed with respect to  
 132 height  $z$ . The PL neither satisfies the upper boundary nor the lower boundary conditions. In compare to log law  
 133 model it fits well for the wind speed profile at larger height, which is one of the critical reason for its preference.  
 134 Though, it had not been recommended to use it very close to the ground. Most of the research matched well with the  
 135 PL over the height value from 30m to 300m a.g.l. The value of  $\alpha$  varies with respect to wind speed, height and  
 136 surface roughness. In practice, the wind shear exponent  $\alpha$  often assumed as equivalent to the aerodynamic roughness  
 137 length  $z_o$ .

#### 138 **2.4 Estimation of Monin-Obukhov length**

139 The turbulence within the surface boundary layer is defined by Monin- Obukhov length scale  $L$  as:

$$140 \quad L = - \frac{\rho C_p T u_*^3}{k g H} \quad (9)$$

141 where  $\rho$  stands for air density at temperature  $T$ ,  $C_p$  is the specific heat at constant pressure,  $k$  is the Von Karman  
 142 constant  $u_*$  is the friction velocity and  $H$  is the sensible heat flux. The Monin- Obukhov length scale  $L$  can be  
 143 calculated by computing the Bulk Richardson number which requires only single wind speed and temperature  
 144 measurements at two heights. Gradient and bulk Richardson number can be defined as:

$$145 \quad R_i = \frac{g \Delta z \Delta \theta}{\theta_1 \Delta u^2} \quad (10)$$

146 where  $\Delta \theta = \theta_2 - \theta_1$ ,  $\Delta z = z_2 - z_1$  and  $\Delta u = u_2 - u_1$  are the measured parameter at two height. When the temp. and wind  
 147 speed measurement is available only at single height (Barker and Baxter, 1975)

$$148 \quad R_{ib} = \frac{g z_2 \Delta \theta}{\theta_2 u_2^2} \quad (11)$$

$$149 \quad \varepsilon = \frac{\varphi_m^2}{\varphi_h} R_i \text{ (Businger et.al., 1971) suggested} \quad (12)$$

150  $\frac{\bar{z}}{L} = \varepsilon$ ,  $\bar{z}$  stands for geometrical mean height of  $z_1$  and  $z_2$ , and  $\varphi_m$  and  $\varphi_h$  are the non dimensional functions related to  
 151 Wind shear and temperature gradient, as per (Dyer, 1974)  $\varphi_m$  and  $\varphi_h$  :

$$152 \quad \varphi_m = \begin{cases} (1 - \gamma \varepsilon)^{\frac{1}{4}}, & \varepsilon < 0 \\ (1 + \beta \gamma), & \varepsilon \geq 0 \end{cases} \quad (13)$$

$$153 \quad \varphi_h = \begin{cases} R(1 - \gamma \varepsilon)^{\frac{1}{2}}, & \varepsilon < 0 \\ (R + \beta \gamma), & \varepsilon \geq 0 \end{cases} \quad (14)$$

154 (Binkowski, 1975) found the following results, the function based on two stability conditions

$$155 \quad \varepsilon = \begin{cases} \frac{R_i}{R} (1 - \gamma R_i)^{\frac{1}{2}} / (1 - \gamma R_i)^{\frac{1}{2}} & R_i \leq 0 \\ \frac{R_i}{R} & 0 < \frac{R_i \beta^2}{\beta} < 1 \end{cases} \quad (15)$$

$$156 \quad \bar{z} = \frac{z_1 + z_2}{2}, \quad \bar{z} \text{ is the mean height} \quad (16)$$

$$158 \quad \frac{z_2}{L} = \frac{k R_{ib} F^2}{G} \quad (17)$$

$$159 \quad F = \frac{u}{u_*} \begin{cases} \ln \left[ \left( \frac{z_2}{z_o} \right) \left( \frac{\eta_o^2 + 1}{\eta_2^2 + 1} \right) \left( \frac{\eta_o + 1}{\eta_2 + 1} \right)^2 \right] + 2 \tan^{-1} \left( \frac{\eta_o - \eta_2}{1 + \eta_o \eta_2} \right), & L \leq 0 \\ \ln \left( \frac{z_2}{z_o} \right) + \frac{\beta z_2}{L}, & L \geq 0 \end{cases} \quad (18)$$

160  $L$  depends upon two stability conditions



161

$$162 \quad G = \frac{\Delta \theta u_*}{(-w'\theta')} = \begin{cases} R \ln \left[ \left( \frac{z_2}{z_0} \right) \left( \frac{\lambda_1 + 1}{\lambda_2 + 1} \right)^2 \right], & L \leq 0 \\ R \left[ \ln \left( \frac{z_2}{z_0} \right) + \frac{\beta(z_2 - z_1)}{L} \right], & L \geq 0 \end{cases} \quad (19)$$

$$163 \quad \eta_2 = (1 - \gamma z_2 / L)^{\frac{1}{4}} \quad (20)$$

$$164 \quad \eta_0 = (1 - \gamma z_0 / L)^{\frac{1}{4}} \quad (21)$$

$$165 \quad \lambda_1 = (1 - \gamma' z_1 / L)^{\frac{1}{2}} \quad (22)$$

$$166 \quad \lambda_2 = (1 - \gamma' z_2 / L)^{\frac{1}{2}} \quad (23)$$

167 Where  $\eta_2$   $\eta_0$   $\lambda_1$   $\lambda_2$  are the function of Monin- Obukhov length  $L$ .  $G$  is the function of Richardson no. and mean  
 168 gradient height  $z$ .  $F$  stands for logarithmic function of speed and friction velocity.

### 169 3. Observation and site details

170 Jamgodrani hills have a huge potential in terms of power production. The 100m mast is located in District Dewas at  
 171 Jamgodrani Hills. The elevation of the mast location is 573m above mean sea level. Site coordinate has been  
 172 converted into UTM (Universe Transverse Mercator) system to perform line and area roughness calculation purpose  
 173 using WASP and windPRO. There were five wind anemometers and wind vane had mounted on the mast to measure  
 174 wind speed and direction respectively. To verify the Monin- Obukhov Similarity theory two temperatures and one  
 175 pressure sensor had also installed. Table 1 and Fig.1 shows the mast details and location respectively.

176 Table 1 Site Details

Site Coordinate	(E)Longitude- 76°09'2.50" (N) Latitude- 22°58' 58.20" UTM-2542426 N, 619480 E
Duration	2015 to 2017
Site name	Jamgodrani Hills
District	Dewas
State name	Madhya Pradesh
Mast Height	100m
Elevation	573mAMSL
Location of Anemometer	10m, 25m, 50m, 80m, 100m.
Location of Wind vane	10m, 25m, 50m, 80m, 100m
Location of Pressure sensors	2m, 10m
Location of temperature sensors	2m, 10m



177



178

179 Fig. 1 Met mast location (Source Google Earth)

180

181 Weibull parameter (k and c) was calculated by two different methods namely as MLM and MMLM. It is very much  
 182 clear from the Table 3 in compare to Table 2 Weibull parameter are more than Table 2.

183

184 MLM is a widely accepted method to estimate the Weibull parameter. It requires more extensive mathematical  
 185 calculations. In the first step k is calculated by using the following equation.

$$186 \quad k = \left( \frac{\sum_{i=1}^n v_i^k \ln(v_i)}{\sum_{i=1}^n v_i^k} - \frac{\sum_{i=1}^n \ln(v_i)}{n} \right)^{-1} \quad (24)$$

$$187 \quad c = \left( \frac{1}{n} \sum_{i=1}^n v_i^k \right)^{\frac{1}{k}} \quad (25)$$

188 n stands no of observation of zero wind speed and  $v_i$  i<sub>th</sub> operation wind speed.

189

190 This method is similar to MLM and estimated by iteratively using the following two equations . It is used when  
 191 wind data is available in frequency distribution form. If  $v_i$  is the wind speed related to bin i,  $f(v_i)$  is the frequency  
 192 range within the region of bin i, n is the total no of bins and  $f(v \geq 0)$  is the probability of wind speed.

$$193 \quad k = \left( \frac{\sum_{i=1}^n v_i^k \ln(v_i) f(v_i)}{\sum_{i=1}^n v_i^k f(v_i)} - \frac{\sum_{i=1}^n \ln(v_i) f(v_i)}{f(v \geq 0)} \right)^{-1} \quad (26)$$

$$194 \quad c = \left( \frac{1}{f(v \geq 0)} \sum_{i=1}^n v_i^k \right)^{\frac{1}{k}} \quad (27)$$





Table 2 Weibull parameter by MLM

100m		80m		50m		10m	
k	c	k	c	k	c	k	c
2.24	7.131	2.219	6.70	2.3621	6.25	2.164	4.193

Table 3 Weibull parameter by MMLM

100m		80m		50m		10m	
k	c	k	c	k	c	k	c
2.431	7.67	2.42	7.24	2.57	6.78	2.45	4.736

\*Roughness length=0.3183m, \*Class= 2.8

#### 4. Result & Discussion

Annual mean wind speed and Mean turbulence intensity is calculated at different heights from ground level. It is clear from Table 4 that the annual wind speed increase with respect height, but mean turbulence intensity decreases. Due to more predominate viscous and obstruction effect near the ground level wind turbulence is more. As the height from the ground increases wind becomes so smooth cause rapidly decrease in TU.

Table 4 Wind characteristics

AMWS (Annual Mean wind speed) in m/s				MEAN TURBULANE INTENISTY (TU)			
100m	80m	50m	10m	100m	80m	50m	10m
6.32	5.93	5.53	3.71	0.124	0.143	0.150	0.24

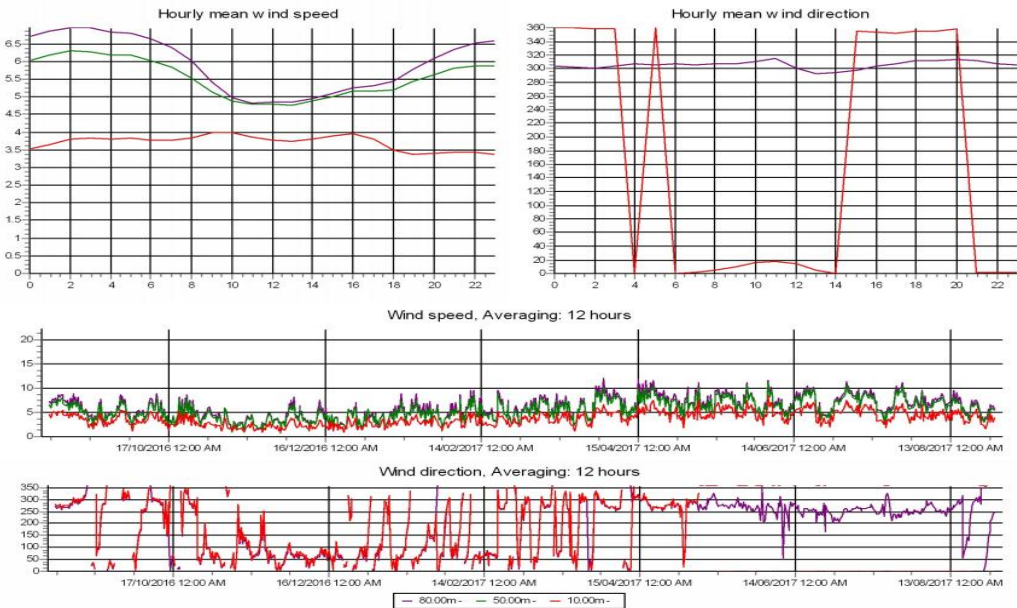
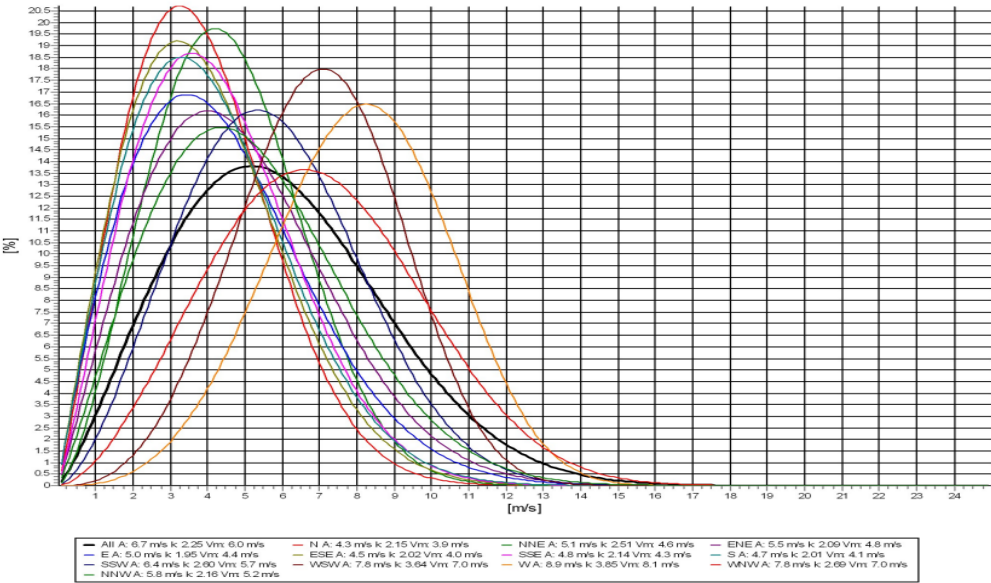


Fig. 2 Wind speed and direction variation





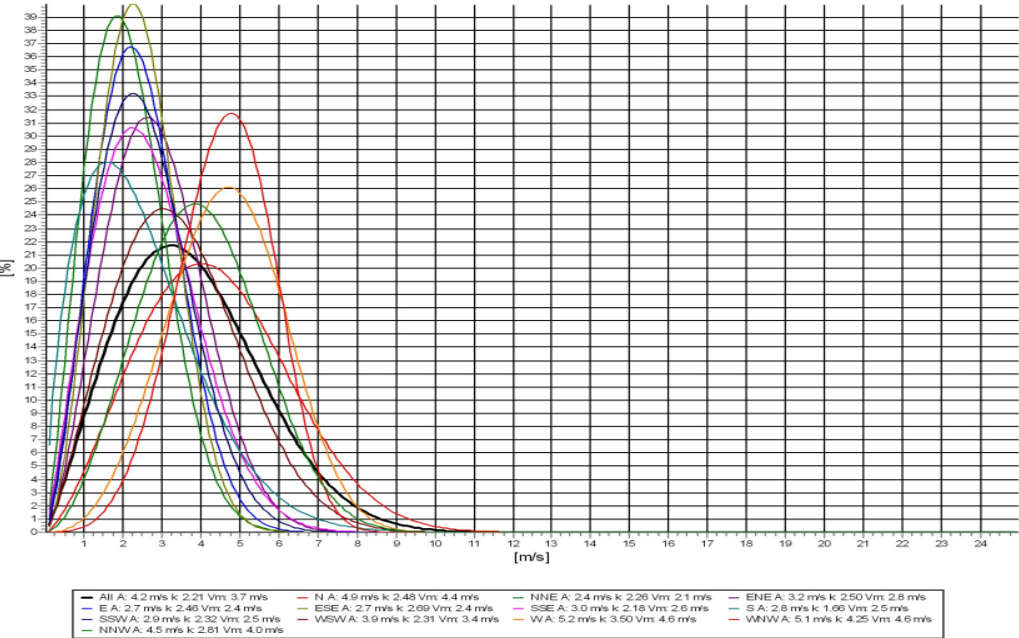
208 The hourly variation of wind speed and direction has been shown in Fig. 2 at 10m, 50m and 80m height  
209 respectively.



210

211

Fig. 3 Sector wise Weibull parameter distribution at 80m height a.g.l.



212

213

Fig. 4 Sector wise Weibull parameter distribution at 10m height a.g.l.



Fig.3 and Fig. 4 shows the sector wise distribution of Weibull parameter at 80m and 10m height respectively.

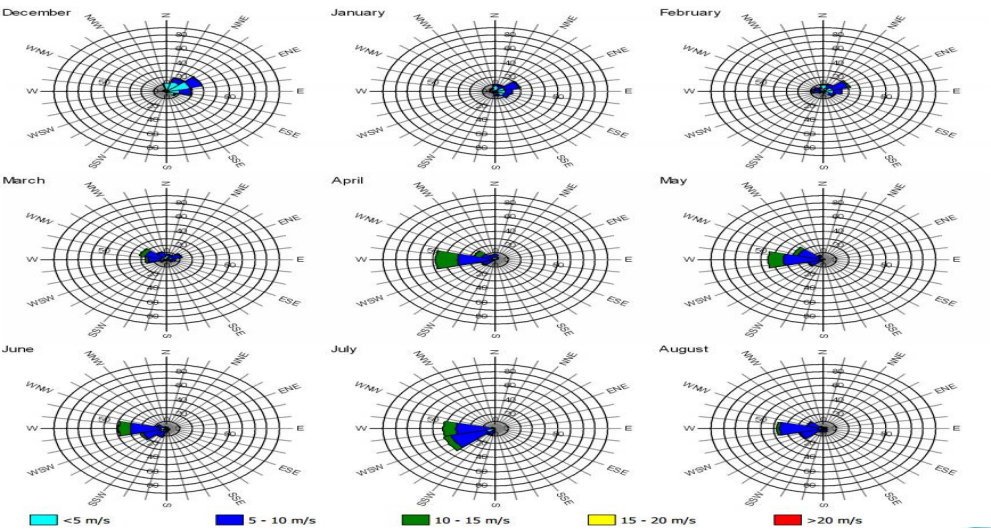


Fig. 5 Energy rose at 80m height

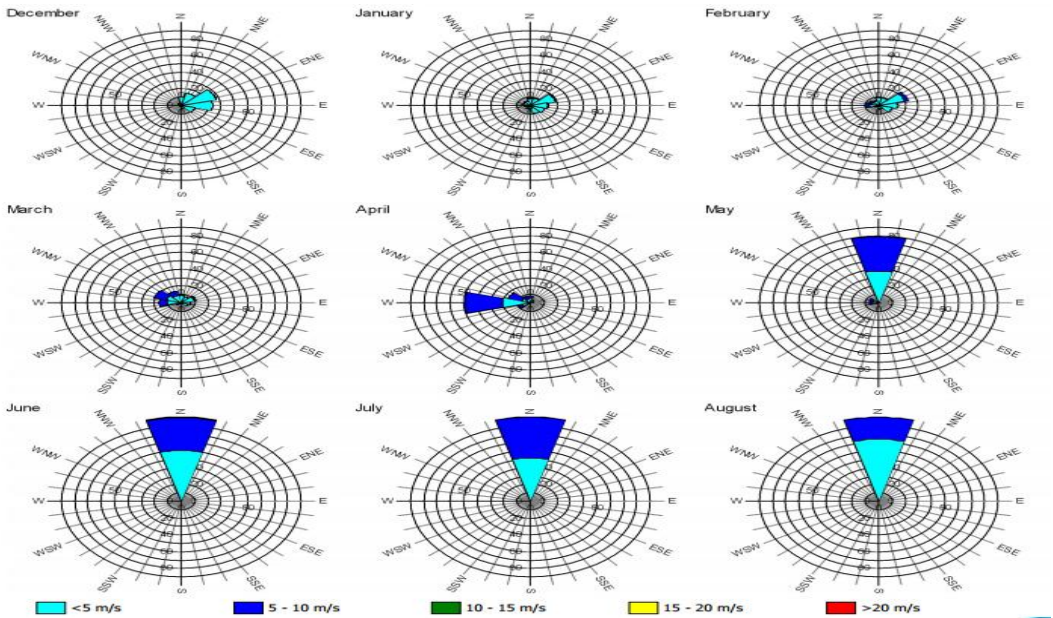


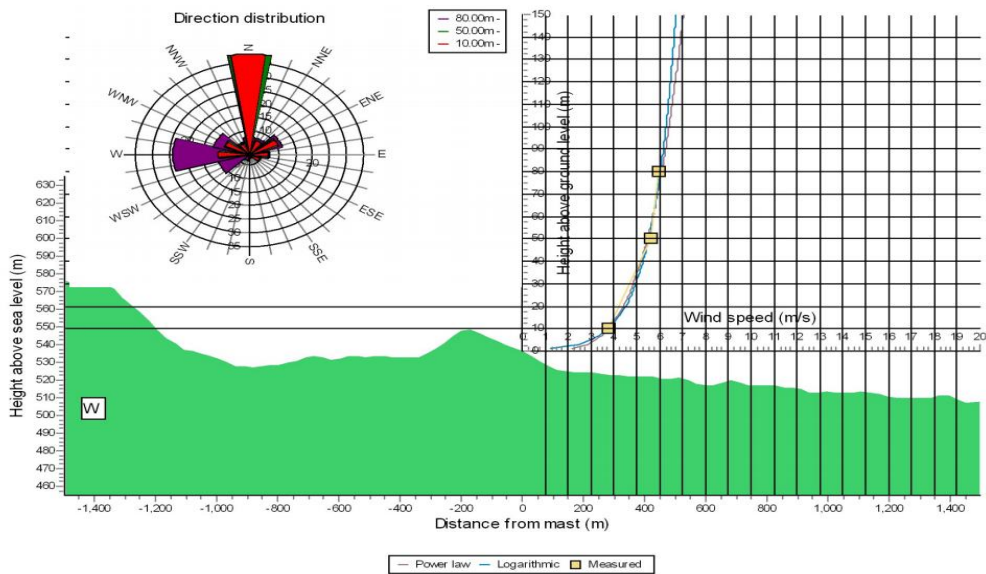
Fig. 6 Energy rose at 10m height



In Fig. 5 (April month) upto 20m/s wind speed has been shown, which produces maximum power density at 80m height. While Fig. 6 indicates that the maximum wind speed can be utilized for the power production is 3 -5 m/s at 10m height. The measured wind speed at 10m a.g.l. can be taken as reference purpose. Further Wind speed has been extrapolated using PL from 50m to 100m and 80m to 100m by  $\alpha_{10-50} = 0.2483$  and  $\alpha_{50-80} = 0.1474$  respectively. By taking the surface length of  $z_0$  0.3183m, von karman factor 0.4 and friction velocity  $u^* 0.4316$  m/s the wind speed can be found using LogL at 100m a.g.l as 6.20m/s.

The Monin- Obukhov Length similarity had been applied at Jamogadrani hills which predict that the atmosphere is strongly stable and wind speed using D&H model found to be 6.68m/s. The Richardson Number is 0.35614 which has been used to calculate Monin- Obukhov scale.

231



232

233 Fig. 7 Mean wind profile using power law and LogL respectively

234 Table 5 Comparative analysis between different models

235

Parameter/Results	Predicted by PL ( $\alpha_{10-50} = 0.2483$ )	Predicted by PL ( $\alpha_{50-80} = 0.1474$ )	LogL	D&H model
Wind speed in m/s	6.580	6.135	6.204	6.681
RMSE	0.26398	0.18085	0.111701	0.36485
NRMSE	0.04094	0.02905	0.017842	0.056139

236

237 It is clear from Table 5 that Log law fitted and best matches the wind profile. RMSE and NRMSE found to be least  
238 in case of Log law in compare to PL and D&H model. The actual measured wind speed by wind anemometer is 6.32  
239 m/s at 100m a.g.l. It can be seen from Fig. 7 that the accuracy of the LogL increases from the height above 80m  
240 a.g.l.

241



## 242 243 **5. Conclusion**

244 To validate its reliability as a wind speed prediction extrapolations tool for addressing MW WTs, the PL, LogL and  
245 D&H model was assessed at hub heights at 10m, 50m, 80m and 100m. Based on a one year data (2016-2017) of 10  
246 min. observations including temperature and pressure data from the Met mast of Jamgodrani hills, all models were  
247 compared. The application of model has required prior assessment of sites surface parameter such as  $\alpha$  for power  
248 law, friction velocity and surface length for Log law and Coriolis factor, ABL height for D&H model. Though,  
249 D&H model was actually developed for strong wind conditions subjected to neutral conditions, it was forced to  
250 applied for all stability regions.

251 The PL, LogL and Deaves and Harris model is outperformed upto height 80m a.g.l. within the extrapolating range.  
252 The results seem to the LogL capability of best producing at higher level. Since, this model has been found to be  
253 suitable for strong adiabatic conditions. However, the overall accuracy of LogL model during these conditions  
254 should be chosen as a model's key factor. Practically, in Indian conditions the DH model could not fit appropriate  
255 due to two limitations: i) reliable friction observation ii) accurate site's surface length assessment. Since, the value  
256 of  $Z_0$  has the major effect on DH model.

257 Based on 10 min. wind speed, pressure and temperature data the minimum RMSE and NRMSE found to be 0.11 and  
258 0.01 respectively. The PL exhibited the more accuracy across all extrapolations ranges and for all stability criteria,  
259 which is used particularly in predicting wind speed profile variation. Currently, obtained results strongly encourage  
260 further uses of the PL, which would be deemed as a future research topic from a wind energy scenario. At  
261 Jamgodrani hills LogL proved to be the finest in prediction the extrapolated wind speed, thus supporting its validity  
262 over the entire ABL.

## 263 **References**

- 264 Barker, E. H., Baxter, T. L., 1975. A note on the computation of atmospheric surface layer fluxes for use in  
265 numerical modeling. J. Appl. Met. 14, 620-622.
- 266 Binkowski, F. S. 1975. On the empirical relationship between the Richardson number and the Monin-Obukhov  
267 stability parameter. Atmospheric Environmental, 9, 453-454.
- 268 Businger, J. A., Wyngaard J. C, Izumi Y. and Bradley E. F. 1971. Flux- profile relationships in the atmospheric  
269 surface layer. J. Atmos. Sci. 288, 181-189.
- 270 Cook, Nicholas J., 1997. The Deaves and Harris ABL model applied to heterogeneous terrain. Journal of Wind  
271 Engineering and Industrial Aerodynamics. 66 (1991) 197-214.
- 272 Counihan, J., 1975. Adiabatic atmospheric boundary layers: a review and analysis of data from the period 1880–  
273 1972. Atmos. Environ. 9, 871–905. [http://dx.doi.org/10.1016/0004-6981\(75\)90088-8](http://dx.doi.org/10.1016/0004-6981(75)90088-8).
- 274 Davenport, A., 1960. Rationale for determining design wind velocities. Journal of Structural Engineering, ASCE  
275 86, 39–68.
- 276 Deaves, D., 1981. Computations of wind flow over changes in surface roughness. Journal of Wind Engineering and  
277 Industrial Aerodynamics 7, 65–94.
- 278 Deaves, D., Harris, R., 1978. A Mathematical model of the structure of strong winds. Report 76. Construction Industry  
279 Research and Information Association.
- 280 Drew, Daniel R., Barlow, Janet F., Lane, Siân E., 2013. Observations of wind speed profiles over Greater London,  
281 UK, using a Doppler lidar. J. Wind Eng. Ind. Aerodyn. 121(2013)98–105.
- 282 Dyer, A., 1974. A review of flux-profile relationships. Boundary-Layer Met. 7, 363-312.
- 283 Elliott, W., 1958. The growth of the atmospheric internal boundary layer. American Geophysical Union 39, 1048–  
284 1054.
- 285 Gualtieri, Giovanni., Secci, Sauro., 2011. Comparing methods to calculate atmospheric stability-dependent wind  
286 speed profiles: A case study on coastal location. Renewable Energy 36 (2011) 2189-2204



287 Gualtieri, Giovanni., 2017. Wind resource extrapolating tools for modern multi-MW wind turbines: Comparison of  
 288 the Deaves and Harris model vs. the power law. *Journal of Wind Engineering & Industrial Aerodynamics* 170  
 289 (2017) 107–117.  
 290 Gualtieri, Giovanni., 2016. Atmospheric stability varying wind shear coefficients to improve wind resource  
 291 extrapolation: A temporal analysis. *Renewable Energy* 87 (2016) 376-390.  
 292 Kikumoto, Hideki., Ooka, Ryozi., Sugawara, Hirofumi., Lim, Jongyeon., 2017. Observational study of power-  
 293 law approximation of wind profiles within an urban boundary layer for various wind conditions. *Journal of Wind*  
 294 *Engineering & Industrial Aerodynamics* 164 (2017) 13–21.  
 295 Panofsky, H., Dutton, J., 1984. *Atmospheric Turbulence: Models and Methods for Engineering Applications*. Wiley.  
 296 Simiu, E., Scanlan, R., 1996. *Wind effects on structures fundamentals and applications to design*. John Wiley and Sons  
 297 Inc.  
 298 Sharma, Pramod Kumar., Baredar, Prashant V. 2017. Analysis on piezoelectric energy harvesting small scale device  
 299 – a review . <https://doi.org/10.1016/j.jksus.2017.11.002>.  
 300 Sharma, Pramod Kumar., Warudkar, Vilas., Ahmed, Siraj. 2014. Experimental investigation of Al 6061/ Al<sub>2</sub>O<sub>3</sub>  
 301 Composite and Analysis of its mechanical properties on onshore wind tower using hybrid technique for Indian  
 302 Condition. *Procedia Materials Science* 5 (2014 ) 147 – 153.  
 303 Sharma et.al., 2014. A Review on Electromagnetic Forming Process.” *Procedia Materials Science* 6 ( 2014 ) 520 –  
 304 527.  
 305 Sharma, Pramod Kumar., Warudkar, Vilas., Ahmed, Siraj. 2014. Design and Optimization of 150 m Higher Wind  
 306 Monitoring Tower (Indian Condition). *International Journal of Scientific Engineering and Technology*. (ISSN :  
 307 2277-1581). 2014 Volume No.3 Issue No.2, pp : 85 – 89.  
 308 Tieleman, Henry W., 2008. Strong wind observations in the atmospheric surface layer. *Journal of Wind Engineering*  
 309 *and Industrial Aerodynamics* 96 (2008) 41–77.  
 310  
 311  
 312  
 313  
 314  
 315  
 316  
 317  
 318  
 319  
 320  
 321  
 322